

## Original Article

# Lidocaine-induced neurotoxicity via upregulating TMEM16F (ano6)

Hailiang Du<sup>1</sup>, Xinyuan Liu<sup>2</sup>, Wei Gao<sup>1</sup>, Shuyuan Liu<sup>1</sup>, Yaomin Zhu<sup>1</sup>

<sup>1</sup>Department of Anesthesiology, The First Affiliated Hospital of Xi'an Jiaotong University, Xi'an, Shaanxi, People's Republic of China; <sup>2</sup>Department of Nursing, The Second Affiliated Hospital of Xi'an Jiaotong University, Xi'an, Shaanxi, People's Republic of China

Received June 1, 2020; Accepted September 29, 2020; Epub December 15, 2020; Published December 30, 2020

**Abstract:** Purpose: The aim of this study was to investigate the possible mechanism of lidocaine neurotoxicity. Methods: Forty rats were randomly divided into four groups: the control, sham, saline, and lidocaine groups. Neurobehavioral tests were performed on rats in each group before and 1-4 days after the intrathecal administration. On the fourth day, the spinal cords of all rats from L2 to L6 were taken out and immediately stored in liquid nitrogen. In the control and lidocaine groups, parts of the spinal cord tissues of three rats in each group were selected for gene microarray analysis, revealing that compared with the control group, TMEM16F (ano6) expression was upregulated in the lidocaine group. To verify the expression of ano6 at the mRNA and protein levels, five rats in each group underwent real-time quantitative polymerase chain reaction (RQ-PCR) and five underwent western blot analysis. The SK-N-SH cells were cultured and randomly assigned into control, lidocaine, and ano6 siRNA + lidocaine groups. The expression level of ano6 in each group was detected, and flow cytometry was used to detect apoptosis. Results: The expression of ano6 in spinal cord neurons was up-regulated for lidocaine neurotoxicity and induced neurobehavioral changes in rats. Knockdown of ano6 could alleviate the apoptosis of neurons induced by lidocaine. Conclusions: Neuronal apoptosis induced by lidocaine neurotoxicity might be due to the upregulation of ano6 expression. Inhibition of ano6 expression alleviated the apoptosis induced by lidocaine neurotoxicity.

**Keywords:** Neurotoxicity, apoptosis, lidocaine, TMEM16F (ano6)

## Introduction

Represented by lidocaine, local anesthetics (LAs) are widely used to induce regional and intraspinal anesthesia [1, 2]. The mechanism of LAs is mainly to block the voltage-gated sodium channel of neurons reversibly, thereby blocking the transmission of nerve impulses [3]. The complications caused by LA neurotoxicity, such as transient neurologic symptoms and cauda equina syndrome, are rare, but usually with severe outcomes. The mechanism of LA neurotoxicity has always been the focus of research, but the "overall view" is still unclear [4].

Previous reports have shown that lidocaine is highly neurotoxic among commonly used LAs [5-7]. Now, gene chip technology is widely used to screen a variety of differentially expressed genes. Through this technology, the differentially expressed genes caused by lidocaine neu-

rotoxicity in the position regulation of apoptotic process were detected and verified. Cell experiments were conducted to investigate the potential mechanism of lidocaine neurotoxicity.

## Material and methods

### Ethical assessment

In the present study, all the plans were examined and approved by the Animal Research and Ethics Committee of the First Affiliated Hospital of Xi'an Jiaotong University, Shaanxi Province. All technical processes were implemented following the Principles of the Helsinki Declaration.

### Animals

The experimental animals were produced by the experimental animal center of the Medical College of Xi'an Jiaotong University. They included 40 rats of 260-280 g, which were all male Sprague Dawley rats. The animals were fed at

## Lidocaine neurotoxicity and TMEM16F (ano6)

room temperature ( $25 \pm 1^\circ\text{C}$ ), the light-dark cycle was 12 h and the relative humidity was 40%-60%. The animals were given standard rat feed and water at will and kept individually. They were randomly split into four groups: control group; sham group, received only intrathecal catheter insertion; saline group, saline was injected intrathecally; and lidocaine group, 10% lidocaine was injected intrathecally ( $n = 10$  per group).

### *Intrathecal catheter insertion*

Reference to previous studies, intrathecal catheterization was executed [2]. In brief, the injection of 10% chloral hydrate at the dose of 300-350 g/kg intraperitoneally was used to anesthetize rats. After the intervertebral space of L4-L5 and ligamentum flavum were exposed, a heat-connected polyethylene catheter was inserted 2 cm within the subarachnoid space. Hind leg twitching or tail swing indicated that the catheter was inserted, and the cerebrospinal fluid outflowing indicated its successful insertion. Then, 10  $\mu\text{L}$  of saline was used to flush the catheter. Before suturing the incision, the end of catheter was sealed off and subcutaneously fastened. Once the rats were awake after anesthesia, their movement and clamped foot were monitored to detect any nerve injury caused by the intubation process. The rats with nerve injury were excluded. One day after catheterization, the rats in each group, except group C, were injected with 20  $\mu\text{L}$  of 1% lidocaine intrathecally. The lidocaine screening test was positive for the paralysis of both lower limbs within 30 s. The exclusion criteria were as follows: paralysis of limbs, dyskinesia, negative lidocaine test, or paralysis of unilateral limbs after a puncture. Three rats were excluded and three others supplemented.

### *Intrathecal drug injection*

Behavioral tests were conducted 1 day after catheterization. Then, each rat in the saline group was injected 20  $\mu\text{L}$  of saline into the subarachnoid space. Each rat in the lidocaine group was injected with 20  $\mu\text{L}$  of 10% lidocaine (L5647-15G, Sigma, MO, USA), diluted with saline, into the intrathecal space [2]. Subsequently, 10  $\mu\text{L}$  of saline was used to flush the catheter. The saline and lidocaine solutions were injected manually at a rate of about 10  $\mu\text{L}/15$  s through a microinjector (Shanghai

Gaopigeon Industry and Trade Co. Ltd., China) at a single dose.

### *Neurobehavioral tests*

A researcher who did not aware of the experimental conditions fulfilled all neurobehavioral tests in rats. The sensory and motor functions of rats in each group were measured using the thermal withdrawal latency (TWL) and the score of hindlimb motor dysfunction. A thermal stimulator (PL-200, Chengdu Taimeng Software Co. Ltd., China) was used to measure TWL. Under a 3 mm thick glass plate was a plexiglass box. After the rats were placed on the glass plate quietly, one third of the anterolateral part of the hind sole of the rats was irradiated with the thermal stimulator. TWL was the time between the beginning of irradiation and the occurrence of leg-raising avoidance in rats. The longest time of irradiation was 30 s to prevent tissue damage. TWL was measured five times at 5-min intervals, and the test results of each rat were taken as the average value of five tests. The standard for evaluating hindlimb motor dysfunction was as follows: hindlimbs could move independently, gait was steady and could bear weight, score 0; hindlimbs could not bear weight, gait was not steady, and when pressed or clamped, the hindlimbs had evasive reactions, score 1; hindlimbs could not move independently and when pressed or clamped, no evasive reaction occurred in the hindlimbs, score 2. Neurobehavioral tests were performed in each group before injection (T0) and 1 day (T1), 2 days (T2), 3 days (T3), and 4 days (T4) after the intrathecal injection.

### *Tissue preparation*

The fourth day after subarachnoid injection, neurobehavioral tests were performed on rats in each group. Then, the injection of 10% chloral hydrate at the dose of 300-350 g/kg intraperitoneally was used to anesthetize rats. The spinal cords (lumbar enlargement) of all rats from L2 to L6 were taken out and immediately stored in liquid nitrogen.

### *Microarray analysis and hierarchical clustering*

Parts of spinal cord tissues of three rats were randomly selected from both the control and lidocaine groups for microarray analysis. The TRIzol reagent (Life Technologies, CA, USA)

and the RNeasy mini kit (Qiagen, CA, USA) were successively used to extract and purify the total RNA of spinal cord tissues. According to the standard Affymetrix protocol, an Ambion WT Expression Kit was utilized to prepare the biotinylated cDNA from 150 ng total RNA. Fragmented cDNA was labeled and then hybridized on the gene chip Affymetrix Clariom D rat array (Affymetrix) at 45°C for 16 h. After that, the Affymetrix Fluidics Station 450 was chosen to wash and stain the gene chips. All chips were scanned with the Affymetrix GeneChip Operating Software (GCOS) installed in a GeneChip Scanner 3000 7G. Robust multichip analysis (RMA) algorithm was used for data analysis, and methods of normalization were global scaling and Affymetrix default analysis settings. The values were presented as  $\log_2$  RMA signal intensity. Differentially expressed genes between the two groups were discerned basing on the results of the Student *t* test. The identification criteria for the up- and downregulation of genes were as follows: a fold change > 1.5 and a *P* value < 0.05. The hierarchical clustering tab, an effective way to analyze various large genome datasets, was used for the hierarchical clustering of data. The correlation between samples was calculated by the expression of selected differentially expressed genes. Similar samples were clustered, and the genes in the same cluster had similar biological functions. The Cluster\_Treeview software developed by Stanford University (CA, USA) was used for hierarchical clustering based on differentially expressed mRNA.

### *GO enrichment analysis*

Gene Ontology Database, commonly known as the GO database, which is a cross-species, comprehensive, and descriptive database. The GO enrichment analysis annotated the differentially expressed genes based on the GO database and obtained all the functions of gene participation. Then, Fisher's exact and multiple comparison tests were chosen to compute the significance level (*P* value) and the false discovery rate of each function. The criterion of significance screening was the *P* value less than 0.01.

### *Cell culture*

The Stem Cell Bank of Chinese Academy of Sciences kindly provided the human neuroblas-

toma cell line SK-N-SH for this study. All cell lines were cultured in the Hyclone minimum essential medium, added penicillin and streptomycin, each at a concentration of 50 µg/mL, containing 10% fetal bovine serum. All cells were cultured at 37°C in a moist environment containing 5% carbon dioxide.

### *Ano6 inhibition in SK-N-SH*

Ano6 siRNA (sc-96071, Santa Cruz Biotechnology, Inc., TX, USA) or negative control siRNA-A (sc-37007, Santa Cruz Biotechnology, Inc.) was transfected into SK-N-SH cells using Lipofectamine 2000 (11668019, Invitrogen, MA, USA) in the light of the manufacturer's protocol. Transfection occurred when the cell growth covered 80% of the bottom of the Petri dish (60 mm in diameter). After 48 h of siRNA transfection, the knockdown efficiency was evaluated with RQ-PCR and western blot analysis.

### *SK-N-SH exposed to lidocaine*

After successful ano6 siRNA transfection, the cells cultured under the same conditions were divided into three groups: control, lidocaine, and ano6 siRNA + lidocaine (exposed to lidocaine after knockdown of ano6). The cells in the lidocaine and ano6 siRNA + lidocaine groups were cultured in fresh culture medium containing lidocaine (7.1 mM, L5647-15G, Sigma, MO, USA) referring to the result of a previous study [8], which concentration could establish the early apoptosis model of nerve cells, while those in the control group were cultured in fresh culture medium and served as a negative control. The three groups of cells were cultured for 24 h in the same environment. Afterwards, western blot analysis and RQ-PCR were used to appraise the expression of ano6 in each group, and the apoptotic rate was evaluated with flow cytometry.

### *RNA extraction and RQ-PCR*

The TRIzol reagent (Life Technologies) was chosen to extract the total RNA from spinal cord tissue and SK-N-SH cells for RQ-PCR in the light of the manufacturer's protocols. After that, the reverse transcription program of cDNA was implemented by using a RevertAid First Strand cDNA Synthesis Kit (Thermo Fisher Scientific, MA, USA). RQ-PCR was performed with SYBR Premix Ex Taq II (TaKaRa,

Tokyo, Japan). The primers for SK-N-SH cells were ano6(h)-PR (sc-96071-PR, Santa Cruz Biotechnology, Inc.) and glyceraldehyde-3-phosphate dehydrogenase (GAPDH)(h)-PR (sc-35448-PR, Santa Cruz Biotechnology, Inc.), and those for spinal cord tissue were synthesized by Sangon Biotech (Shanghai) Co., Ltd. ([Supplementary Table 1](#)). The  $2^{-\Delta\Delta Ct}$  method was used to count the relative expression level of ano6, with the cycle threshold value standardized with GAPDH as an internal reference.

### Western blot analysis

The radio immunoprecipitation assay buffer containing protein inhibitors (Beyotime, Guangzhou, China) was used to extract the proteins from spinal cord tissues and SK-N-SH cells. After that, they were electrophoresed (30  $\mu$ g/lane) on 10% sodium dodecyl sulfate-polyacrylamide gel and transferred onto polyvinylidene fluoride (PVDF) membranes. At room temperature, the PVDF membranes were immersed for 1 h in a sealed solution (5% skimmed milk), followed by incubation at 4°C overnight with primary antibodies. After incubated at room temperature for 1 h with the horseradish peroxidase (HRP)-conjugated secondary antibody, a chemiluminescent HRP substrate (WBKLS0100, Millipore Corporation, MA, USA) was used to treat the membranes. The signals were visualized with a luminescent image analyzer (Amersham Imager 600, GE Healthcare Bio-Sciences AB, Sweden). The expression levels of ano6 were standardized to those of  $\beta$ -actin. Quantification analysis was implemented through Image Lab software (Bio-Rad, CA, USA). The following were antibodies applied in this procedure: anti- $\beta$ -actin antibody (1:2000, ab8227, Abcam, MA, USA); anti-ano6 antibody (1:2000, PA5-88322, Invitrogen, MA, USA); and goat anti-rabbit immunoglobulin G (IgG) H&L (HRP) (1:10000, ab6721, Abcam).

### Flow cytometry analysis

An Annexin V-phycoerythrin (PE)/7-amino-actinomycin D (7-ADD) apoptosis detection kit (KGA1018, Jiangsu Kaiji Biotechnology Co., Ltd., China) was utilized to assess the apoptotic ratio of cells in each group. In the light of manufacturer's protocols, the following was the operation procedure: SK-N-SH cells in each group were digested with trypsin without EDTA and collected in centrifugal tubes. Cold phos-

phate-buffered saline was utilized to wash the cells twice. Then, adding 5  $\mu$ L of 7-ADD dye solution to 50  $\mu$ L of binding buffer and mixed. Further, the solution was mixed in each sample and kept in dark place at room temperature for 10 min. After that, 1  $\mu$ L of Annexin V-PE dye solution and 450  $\mu$ L of binding buffer were added to each sample cell, mixed, and kept away from light at room temperature for 10 min. Flow cytometry (BD FACSCanto II; BD Biosciences, CA, USA) with BD Diva software installed immediately was used to analyze the percentages of apoptotic cells within 1 h. For each sample, at least 10,000 cells were analyzed, and the experiment was repeated three times for each group.

### Statistical analyses

The mean  $\pm$  standard error was used to express the measurement data of normal distribution. One-way analysis of variance followed by the least significant difference test was applied to assess the diversities among groups. The grade data of non-normal distribution were expressed as median (quantile range, QR), and the Kruskal-Wallis H test was utilized to compare the differences among groups. A *P* value less than 0.05 was considered to significant statistical difference. The statistical analysis and the creation of all figures were done using SPSS 20.0 (SPSS Inc., IL, USA) and GraphPad Prism 8.0 (GraphPad Software Inc., CA, USA), respectively.

## Results

### *Lidocaine neurotoxicity resulted in the prolongation of TWL in neurobehavioral tests in rats*

No significant difference was found in TWL baseline values among groups before intraspinal injection (T0). On 1-4 days after intrathecal administration, the TWL in the Lido group was significantly longer than in the Con, Sham, and saline groups (*P* < 0.01). Nevertheless, among the Con, Sham, and saline groups, no significant difference was found (*P* > 0.05, **Figure 1**). In motor dysfunction scores of hindlimbs, among the four groups, either before or 1-4 days after intraspinal administration, no significant difference was observed. (*P* > 0.05, [Supplementary Table 2](#)).

## Lidocaine neurotoxicity and TMEM16F (ano6)

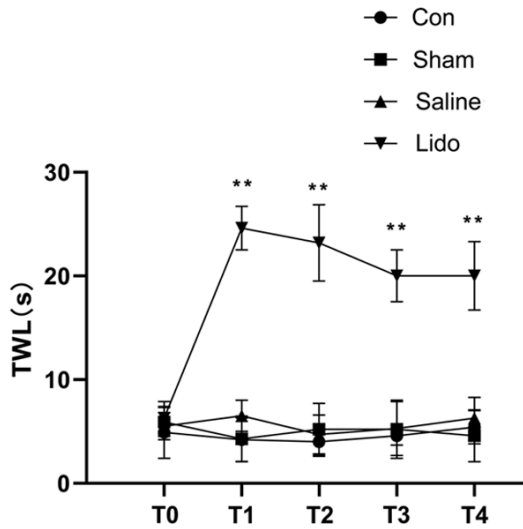


**Figure 1.** TWL test results of rats in each group before intrathecal injection and 1-4 days after the injection. On the first (T1), second (T2), third (T3), and fourth (T4) days after the injection, contrasted with the Con, Sham, and saline groups, the TWL in the Lido group was significantly longer (\*\* $P < 0.01$  vs the Con, Sham, and saline groups,  $n = 10$ ). TWL, Thermal withdrawal latency; T0, before intrathecal injection; and T1-T4: the first, second, third, and fourth day after injection, respectively.

*Microarray, cluster, and GO enrichment analyses showed that contrasted with the Con group, TMEM16F (ano6) expression in the Lido group was upregulated*

Between the Con and Lido groups, the total number of differentially expressed genes was 2316, with 1539 upregulated and 777 downregulated (**Figure 2A**). Unsupervised hierarchical clustering and TreeView analysis were utilized to analyze the data on differentially expressed genes. The differential expression profiles of mRNA between the two groups were displayed through the heat map (**Figure 2B**). Then, the Go analysis was executed on the differentially expressed genes. The GO value was  $-\text{LgP}$  (negative logarithm of  $P$  value), which indicated the correlation between gene expression and related biological processes. A larger  $\text{LgP}$  represented a smaller  $P$  value. The top 10 lidocaine-induced upregulated GOs (upGOs) contained a positive regulation of apoptotic process (**Figure 2C**), and the important gene TMEM16F (ano6) involved in the apoptotic process was upregulated. **Figure 2D** shows the top 10 downregulated GOs. We

have uploaded the microarray data to the NCBI Gene Expression Omnibus (GEO) and GSE136833 is its GEO Series accession number.

*lidocaine upregulating the expression of ano6 was confirmed through RQ-PCR and western blot analysis*

The expression of ano6 of each group was detected by RQ-PCR ( $n = 5$ ) and western blot analysis ( $n = 5$ ) at the mRNA level and protein level, respectively. The results showed that contrasted with the Con, Sham, and saline groups, the relative expression levels of ano6 were significantly higher in the Lido group ( $P < 0.01$ ), while among the Con, Sham, and saline groups, no significant difference was found ( $P > 0.05$ , **Figure 3A** and **3B**).

*Ano6 inhibition in SK-N-SH cells*

RQ-PCR and western blot analysis results showed that transfection of ano6 siRNA effectively knocked down the expression level of ano6 (**Figure 4A** and **4B**). Contrasted with control group, the expression levels of ano6 were significantly higher in the lidocaine group ( $P < 0.01$ ), and in the ano6 siRNA + lidocaine group these levels were significantly lower than the lidocaine group ( $P < 0.01$ , **Figure 4C** and **4D**). This indicated that ano6 siRNA transfection significantly reduced the lidocaine-induced upregulation of ano6 expression.

*Knockdown of ano6 could reduce the apoptosis induced by lidocaine neurotoxicity*

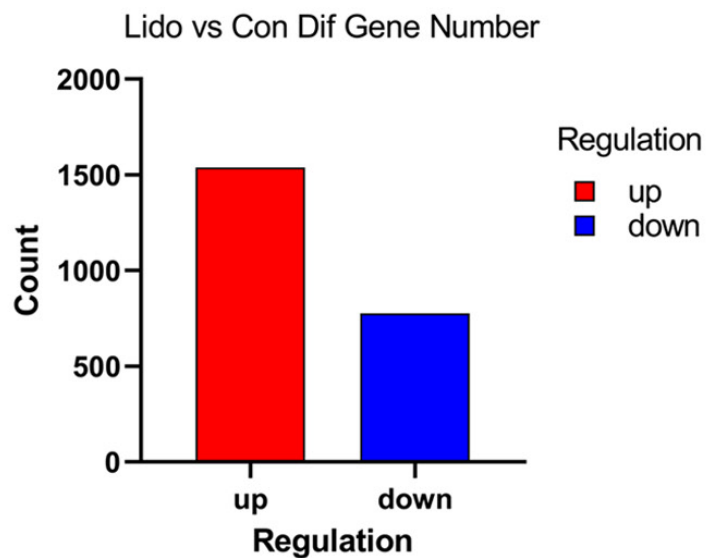
Contrasted with control group, the percentage of apoptotic cells in the lidocaine group was significantly higher ( $P < 0.01$ ), while the ano6 siRNA + lidocaine group was significantly lower than the lidocaine group ( $P < 0.01$ , **Figure 5**). In a word, knockdown of ano6 could reduce neuronal apoptosis induced by the lidocaine neurotoxicity.

## Discussion

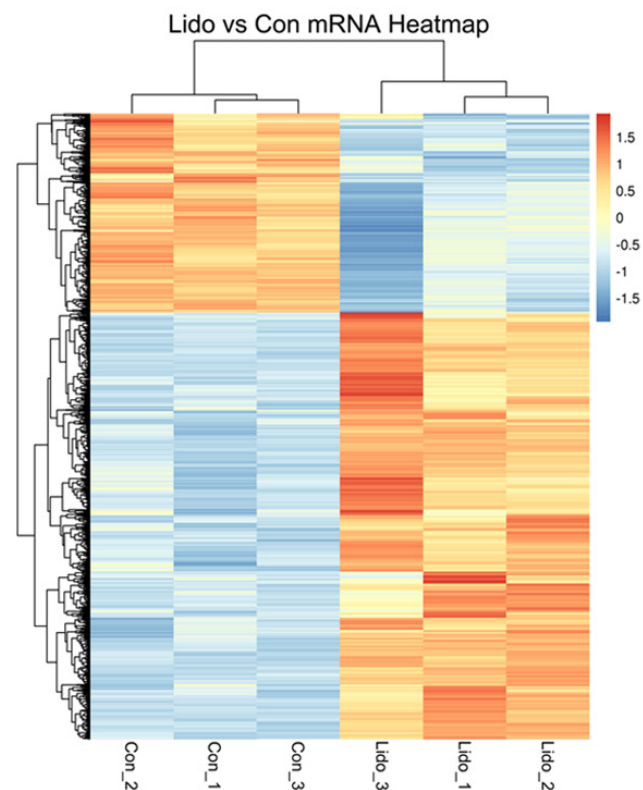
The phospholipids (PS) in the plasmalemma of mammalian cells are not evenly distributed between the two leaflets of the bilayer [9, 10]. Negatively charged PS is distributed mainly in the inner leaflet. The production and maintenance of this asymmetric distribution are due

# Lidocaine neurotoxicity and TMEM16F (ano6)

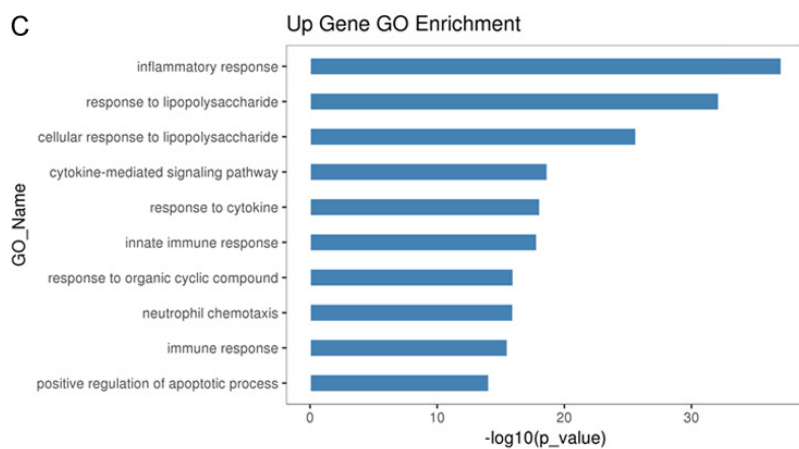
A



B



C



D

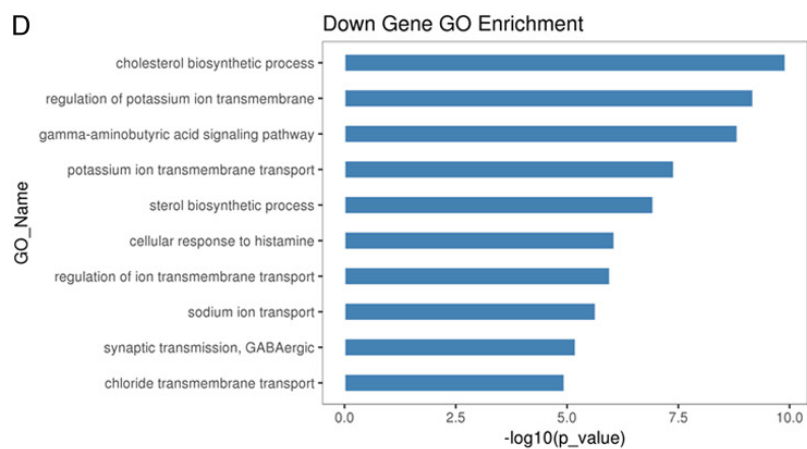


**Figure 2.** Comparison of differentially expressed genes in spinal cord tissue between the control and lidocaine groups. A. Between the Con and Lido groups, the total number of differentially expressed genes was 2316 ( $n = 3$ ; fold change  $> 1.5$ ;  $P < 0.05$ ), with 1539 upregulated and 777 downregulated. B. Hierarchical clustering of differentially expressed mRNAs between the Con and Lido groups. Orange and blue represent upregulated and down-regulated genes, respectively. The GO analysis of differentially expressed mRNA. C. The top 10 upGOs induced by lidocaine comprised the positive regulation of the apoptotic process. D. The top 10 downGOs.

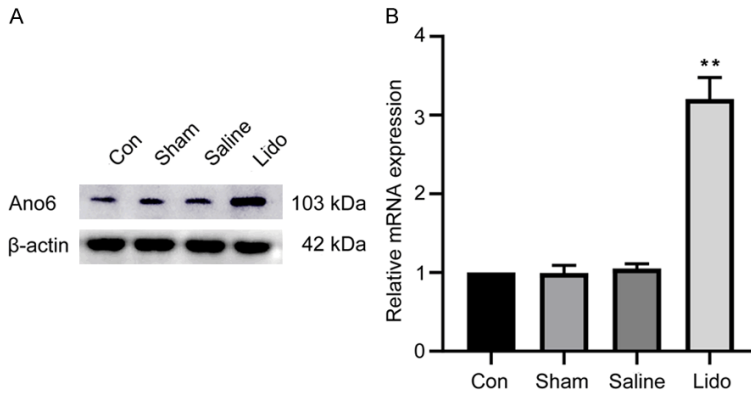


**Figure 3.** Effect of lidocaine on the expression of ano6 in the spinal cord of rats. A. Western blot representative bands of ano6 expression in the spinal cord of rats in each group ( $n = 5$ ). B. RQ-PCR results of the relative expression level of ano6 in each group ( $n = 5$ ). Contrasted with the Con, Sham, and saline groups, the ano6 expression was significantly higher in the Lido group (\*\* $P < 0.01$  vs the Con, Sham, and saline groups).

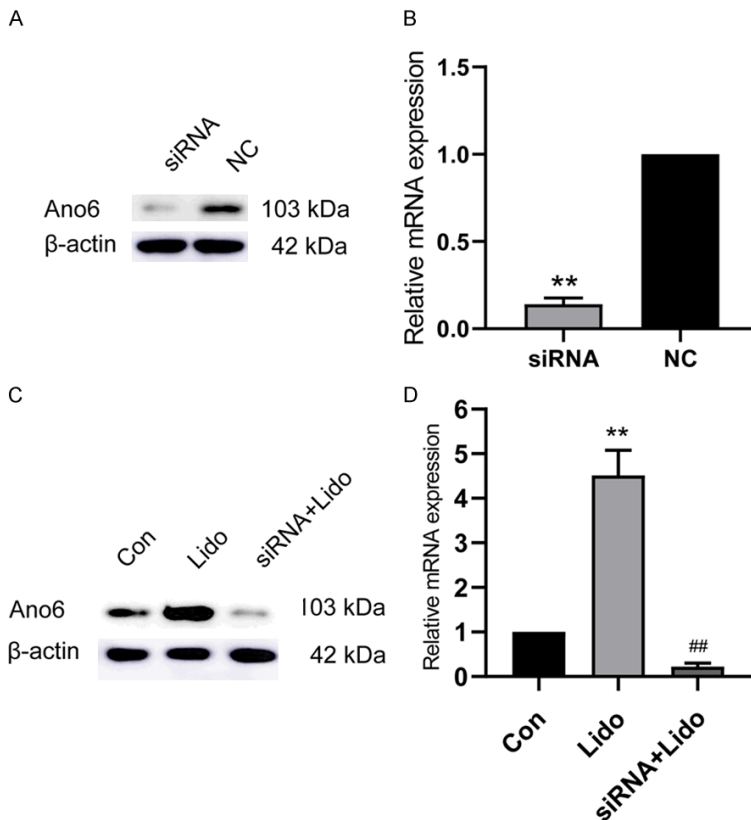


**Figure 4.** Ano6-siRNA transfection significantly reduced the upregulation of ano6 expression induced by lidocaine in SK-N-SH cells. A and B. Western blot

and RQ-PCR analyses of ano6 siRNA knockdown efficiency (\*\* $P < 0.01$  vs negative control siRNA-A). C and D. Western blot and RQ-PCR analyses of ano6 expression level in each group. Ano6-siRNA transfection significantly reduced the upregulation of ano6 expression induced by lidocaine in SK-N-SH cells (\*\* $P < 0.01$  vs Con, ## $P < 0.01$  vs Lido). Typical bands and data from three separate experiments expressed as the mean  $\pm$  SD of each group. NC, negative control siRNA-A group; siRNA, ano6 siRNA group; Con, control group; Lido, lidocaine group; siRNA + Lido, ano6 siRNA + lidocaine group.

to the action of phospholipid translocase (the P4 subfamily of P-type ATPases) [11]. However, under certain conditions, the activation of  $Ca^{2+}$ -dependent “scramblase” can catalyze the rapid externalization of PS on the cell surface to eliminate asymmetry. PS externalization is involved in many important physiological and pathological processes in various types of cells [12]. At present, it is generally believed that PS externalization is a characteristic manifestation of apoptosis [13]. The presence or modification of many proteins and sugar moieties on the surface of apoptotic cells are considered to be the identification signal of phagocytes. However, PS externalization has so far been the best characteristic signal for apoptotic cells to be recognized by phagocytes [14]. PS externalization occurs in the early stages of apoptosis [10, 15], that is, before the

## Lidocaine neurotoxicity and TMEM16F (ano6)

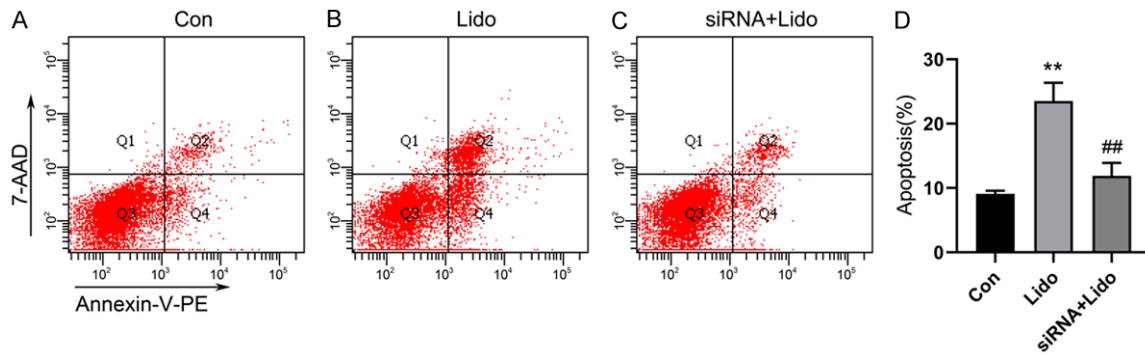


**Figure 5.** Knockdown of ano6 could reduce the apoptosis of SK-N-SH cells induced by lidocaine neurotoxicity. The apoptotic rate was evaluated with flow cytometry. (A-C) Representative images and (D) data from three separate experiments expressed as the mean  $\pm$  SD of each group (\*\* $P < 0.01$  vs Con, ## $P < 0.01$  vs Lido). Con, control group; Lido, lidocaine group; siRNA + Lido, ano6 siRNA + lidocaine group.

loss of membrane integrity or DNA degradation, but after the appearance of membrane blebbing [10].

TMEM16F is a member of the transmembrane protein (TMEM) family, also known as anoctamin 6 (ano6), which has the functions of  $\text{Ca}^{2+}$ -dependent phospholipid scramblase and  $\text{Ca}^{2+}$ -activated chloride channel [16]. However, it is also believed that TMEM16F is only a channel rather than a phospholipid scramblase because the overexpression of ano6 in HEK-293 cells does not result in significant PS externalization [17]. This may be due to cell specificity. Some studies found that ano6 is activated during apoptosis [18, 19]. Forschbach et al. discovered that in the three-dimensional culture of Madin-Darby canine kidney renal cysts, the knockout of ano6 inhibited cell apoptosis [20]. Varied opinions existed about the specific mechanism of ano6 in apoptosis. One view is that the ability of ano6 to scramble membrane phospholipids is may be the mechanism of cell death induced by it [21]. However, Martins et al. hold another view that ano6 promotes apoptosis through its activity as outwardly rectifying  $\text{Cl}^-$  channel (ORCC) because  $\text{Cl}^-$  efflux contributes to cell shrinkage, which is a typical feature of apoptosis [19]. Besides, the activation of ano6-induced apoptosis may also be associated with membrane blebbing [22], membrane shedding [23], and increase in intracellular  $\text{Ca}^{2+}$  concentration. In addition, the present study found that ano6 is also activated in the process of necroptosis, pyroptosis, and ferroptosis [24-28] besides apoptosis. Therefore, some scholars proposed that a novel way to induce cancer cell

death could be achieved by activating ano6 [29].

In the present study, the rats were injected with 10% lidocaine intrathecally to establish a neurotoxic model. Neurobehavioral tests showed that on 1-4 days (T4) after intrathecal administration, the TWL in the Lido group was significantly longer than that in the other groups. It is suggested that lidocaine neurotoxicity of to the sensory impairment of lower limbs in rats, which is consistent with previous findings [2]. However, in motor dysfunction scores of hindlimbs, among the four groups, either before or 1-4 days after intraspinal administration, no significant difference was observed, which is inconsistent with the previous research results [2], this may be the reason of different scoring methods and standards for evaluation. Therefore, it is urgent to establish a unified scoring standard.

The mechanism of LA neurotoxicity has become a hot topic recently. Previous reports have indicated that among commonly used LAs, lidocaine is highly neurotoxic [5-7]. However, some studies have shown no significant difference in neurotoxicity among Las [8, 30]. This inconsistency may be due to different dosage and concentration of administration and different evaluation methods. Recent studies suggest that apoptosis induced by lidocaine neurotoxicity may be due to its effects on the phosphatidylinositol 3-hydroxy kinase (PI3K) pathway [31], intrinsic caspase pathway [32], and mitogen-activated protein kinase (MAPK) pathway [33]. However, as an important apoptosis related protein, the role

of ano6 has not been mentioned. Microarray technology is commonly used to detect differentially expressed genes, which is mostly used in tumor related research, but its application in lidocaine neurotoxicity research has not been reported. In this research, the results of gene chip analysis of the spinal cord tissue of rats indicated that in the lidocaine group, the expression of ano6 related to apoptosis was significantly upregulated, which was confirmed by subsequent gene- and protein-level detection. To further study the role of ano6 in lidocaine-induced neurotoxicity, ano6-siRNA was used to knockdown the expression of ano6 in SK-N-SH cells. The cell experiments showed that lidocaine could significantly upregulate the expression of ano6 and increase the apoptotic rate of SK-N-SH cells. Knockdown of ano6 could alleviate apoptosis induced by lidocaine neurotoxicity. Therefore, apoptosis induced by lidocaine neurotoxicity might be related to the upregulation of ano6 expression. The mechanism might be as follows: (1) Some studies suggested that lidocaine neurotoxicity is related to the increase in intracellular  $Ca^{2+}$  concentration [32]. High intracellular  $Ca^{2+}$  concentration could activate calcium-dependent phospholipid scramblase ano6, thereby increasing the apoptosis caused by facilitating PS externalization. (2) It is now believed that apoptosis induced by lidocaine neurotoxicity is related to a variety of signaling pathways, as mentioned above. However, caspase inhibitors, such as B-cell lymphoma 2, or inhibitors of transcription or translation (blocking apoptotic processes at any stage) can inhibit PS externalization [10]. As an important phospholipid scramblase in the apoptotic process, ano6 may be activated by the apoptotic signaling pathways, as above mentioned, mediated by lidocaine neurotoxicity. That is, the upregulation of ano6 and PS externalization is downstream of these apoptotic signaling pathways.

In conclusion, the neuronal apoptosis induced by lidocaine neurotoxicity might be due to the upregulation of ano6 expression, while knockdown of ano6 could alleviate the apoptosis, which allows new strategy to prevent and treat complications caused by lidocaine neurotoxicity.

### Acknowledgements

The authors thank Beijing Cnkingbio Biotechnology Co., Ltd for assistance in bioinfor-

matics. Supported by Science and Technology Research and Development Program of Shaanxi Province, China (Grant No. 2014KW25-02).

### Disclosure of conflict of interest

None.

**Address correspondence to:** Dr. Yaomin Zhu, Department of Anesthesiology, The First Affiliated Hospital of Xi'an Jiaotong University, 277 West Yanta Road, Xi'an 710061, Shaanxi, People's Republic of China. Tel: +86-18629382846; E-mail: yaomin\_zhu@126.com

### References

- [1] Albalawi F, Lim JC, DiRenzo KV, Hersh EV and Mitchell CH. Effects of lidocaine and articaine on neuronal survival and recovery. *Anesth Prog* 2018; 65: 82-88.
- [2] Zhao G, Li D, Ding X and Li L. Nerve growth factor pretreatment inhibits lidocaine-induced myelin damage via increasing BDNF expression and inhibiting p38 mitogen activation in the rat spinal cord. *Mol Med Rep* 2017; 16: 4678-4684.
- [3] Nau C and Wang GK. Interactions of local anesthetics with voltage-gated  $Na^+$  channels. *J Membr Biol* 2004; 201: 1-8.
- [4] Verlinde M, Hollmann MW, Stevens MF, Hermanns H, Werdehausen R and Lirk P. Local anesthetic-induced neurotoxicity. *Int J Mol Sci* 2016; 17: 339.
- [5] Cherng CH, Wong CS, Wu CT and Yeh CC. Glutamate release and neurologic impairment after intrathecal administration of lidocaine and bupivacaine in the rat. *Reg Anesth Pain Med* 2011; 36: 452-456.
- [6] Takenami T, Yagishita S, Murase S, Hiruma H, Kawakami T and Hoka S. Neurotoxicity of intrathecally administered bupivacaine involves the posterior roots/posterior white matter and is milder than lidocaine in rats. *Reg Anesth Pain Med* 2005; 30: 464-472.
- [7] Sakura S, Kirihara Y, Muguruma T, Kishimoto T and Saito Y. The comparative neurotoxicity of intrathecal lidocaine and bupivacaine in rats. *Anesth Analg* 2005; 101: 541-547.
- [8] Werdehausen R, Fazeli S, Braun S, Hermanns H, Essmann F, Hollmann MW, Bauer I and Stevens MF. Apoptosis induction by different local anaesthetics in a neuroblastoma cell line. *Br J Anaesth* 2009; 103: 711-718.
- [9] Bretscher MS. Asymmetrical lipid bilayer structure for biological membranes. *Nat New Biol* 1972; 236: 11-12.
- [10] Bevers EM and Williamson PL. Phospholipid scramblase: an update. *FEBS Lett* 2010; 584: 2724-2730.

## Lidocaine neurotoxicity and TMEM16F (ano6)

- [11] Nandrot EF, Anand M, Almeida D, Atabai K, Sheppard D and Finnemann SC. Essential role for MFG-E8 as ligand for alphavbeta5 integrin in diurnal retinal phagocytosis. *Proc Natl Acad Sci U S A* 2007; 104: 12005-12010.
- [12] Pedemonte N and Galletta LJ. Structure and function of TMEM16 proteins (anoctamins). *Physiol Rev* 2014; 94: 419-459.
- [13] Suzuki J, Umeda M, Sims PJ and Nagata S. Calcium-dependent phospholipid scrambling by TMEM16F. *Nature* 2010; 468: 834-838.
- [14] Bevers EM and Williamson PL. Getting to the outer leaflet: physiology of phosphatidylserine exposure at the plasma membrane. *Physiol Rev* 2016; 96: 605-645.
- [15] Schlegel RA and Williamson P. Phosphatidylserine, a death knell. *Cell Death Differ* 2001; 8: 551-563.
- [16] Muratori C, Pakhomov AG, Gianulis E, Meads J, Casciola M, Mollica PA and Pakhomova ON. Activation of the phospholipid scramblase TMEM16F by nanosecond pulsed electric fields (nsPEF) facilitates its diverse cytophysiological effects. *J Biol Chem* 2017; 292: 19381-19391.
- [17] Yang H, Kim A, David T, Palmer D, Jin T, Tien J, Huang F, Cheng T, Coughlin SR, Jan YN and Jan LY. TMEM16F forms a Ca<sup>2+</sup>-activated cation channel required for lipid scrambling in platelets during blood coagulation. *Cell* 2012; 151: 111-122.
- [18] Juul CA, Grubb S, Poulsen KA, Kyed T, Hashem N, Lambert IH, Larsen EH and Hoffmann EK. Anoctamin 6 differs from VRAC and VSOAC but is involved in apoptosis and supports volume regulation in the presence of Ca<sup>2+</sup>. *Pflugers Arch* 2014; 466: 1899-1910.
- [19] Martins JR, Faria D, Kongsuphol P, Reisch B, Schreiber R and Kunzelmann K. Anoctamin 6 is an essential component of the outwardly rectifying chloride channel. *Proc Natl Acad Sci U S A* 2011; 108: 18168-18172.
- [20] Forschbach V, Goppelt-Struebe M, Kunzelmann K, Schreiber R, Piedagnel R, Kraus A, Eckardt KU and Buchholz B. Anoctamin 6 is localized in the primary cilium of renal tubular cells and is involved in apoptosis-dependent cyst lumen formation. *Cell Death Dis* 2015; 6: e1899.
- [21] Gyobu S, Ishihara K, Suzuki J, Segawa K and Nagata S. Characterization of the scrambling domain of the TMEM16 family. *Proc Natl Acad Sci U S A* 2017; 114: 6274-6279.
- [22] Ousingsawat J, Wanitchakool P, Kmit A, Romao AM, Jantarajit W, Schreiber R and Kunzelmann K. Anoctamin 6 mediates effects essential for innate immunity downstream of P2X7 receptors in macrophages. *Nat Commun* 2015; 6: 6245.
- [23] Bricogne C, Fine M, Pereira PM, Sung J, Tijani M, Wang Y, Henriques R, Collins MK and Hilgemann DW. TMEM16F activation by Ca(2+) triggers plasma membrane expansion and directs PD-1 trafficking. *Sci Rep* 2019; 9: 619.
- [24] Schreiber R, Ousingsawat J, Wanitchakool P, Sirianant L, Benedetto R, Reiss K and Kunzelmann K. Regulation of TMEM16A/ANO1 and TMEM16F/ANO6 ion currents and phospholipid scrambling by Ca(2+) and plasma membrane lipid. *J Physiol* 2018; 596: 217-229.
- [25] Ousingsawat J, Cabrita I, Wanitchakool P, Sirianant L, Krautwald S, Linkermann A, Schreiber R and Kunzelmann K. Ca(2+) signals, cell membrane disintegration, and activation of TMEM16F during necroptosis. *Cell Mol Life Sci* 2017; 74: 173-181.
- [26] Ousingsawat J, Wanitchakool P, Schreiber R and Kunzelmann K. Contribution of TMEM16F to pyroptotic cell death. *Cell Death Dis* 2018; 9: 300.
- [27] Ousingsawat J, Schreiber R and Kunzelmann K. TMEM16F/Anoctamin 6 in ferroptotic cell death. *Cancers (Basel)* 2019; 11: 625.
- [28] Kunzelmann K. Ion channels in regulated cell death. *Cell Mol Life Sci* 2016; 73: 2387-2403.
- [29] Kunzelmann K, Ousingsawat J, Benedetto R, Cabrita I and Schreiber R. Contribution of anoctamins to cell survival and cell death. *Cancers (Basel)* 2019; 11: 382.
- [30] Lirk P, Haller I, Colvin HP, Lang L, Tomaselli B, Klimaschewski L and Gerner P. In vitro, inhibition of mitogen-activated protein kinase pathways protects against bupivacaine- and ropivacaine-induced neurotoxicity. *Anesth Analg* 2008; 106: 1456-1464.
- [31] Ma R, Wang X, Lu C, Li C, Cheng Y, Ding G, Liu L and Ding Z. Dexamethasone attenuated bupivacaine-induced neuron injury in vitro through a threonine-serine protein kinase B-dependent mechanism. *Neuroscience* 2010; 167: 329-342.
- [32] Doan LV, Eydlin O, Piskoun B, Kline RP, Recio-Pinto E, Rosenberg AD, Blanck TJ and Xu F. Despite differences in cytosolic calcium regulation, lidocaine toxicity is similar in adult and neonatal rat dorsal root ganglia in vitro. *Anesthesiology* 2014; 120: 50-61.
- [33] Haller I, Hausott B, Tomaselli B, Keller C, Klimaschewski L, Gerner P and Lirk P. Neurotoxicity of lidocaine involves specific activation of the p38 mitogen-activated protein kinase, but not extracellular signal-regulated or c-jun N-terminal kinases, and is mediated by arachidonic acid metabolites. *Anesthesiology* 2006; 105: 1024-1033.

## Lidocaine neurotoxicity and TMEM16F (ano6)

**Supplementary Table 1.** Quantitative real-time PCR primers

| Gene  | Sequence (5'-3')             |
|-------|------------------------------|
| Ano6  | F: CCGCCACCAGAAGTCGCATTG     |
|       | R: ACAGGAGGTAACGCTCGCTAGG    |
| GAPDH | F: GGTGGACCTCATGGCCTACA      |
|       | R: CTCTCTTGCTCTCAGTATCCTTGCT |

**Supplementary Table 2.** Motor dysfunction score of hindlimbs

| Group  | N  | T0    | T1    | T2    | T3    | T4    |
|--------|----|-------|-------|-------|-------|-------|
| Con    | 10 | 0 (0) | 0 (0) | 0 (0) | 0 (0) | 0 (0) |
| Sham   | 10 | 0 (0) | 0 (0) | 0 (0) | 0 (0) | 0 (0) |
| Saline | 10 | 0 (0) | 0 (0) | 0 (0) | 0 (0) | 0 (0) |
| Lido   | 10 | 0 (0) | 0 (0) | 0 (0) | 0 (0) | 0 (0) |

Values are expressed in median (QR). No significant difference was found in motor dysfunction scores of hindlimbs among the four groups, either before intraspinal administration or 1-4 days after intraspinal administration ( $P > 0.05$ ). Therefore, the intrathecal injection of 10% lidocaine did not cause motor dysfunction in rats. T0, before intraspinal injection; T1, the first day after the injection; T2, the second day after the injection; T3, the third day after the injection; and T4, the fourth day after the injection.